http://dx.doi.org/10.5012/bkcs.2012.33.12.4052

The Synergistic Effect of Nitrogen and Ni_2O_3 over TiO_2 Photocatalyst in the Degradation of 2,4,6-Trichlorophenol Under Visible Light

Shaozheng Hu,* Fayun Li,* and Zhiping Fan

Institute of Eco-environmental Sciences, Liaoning Shihua University, Fushun 113001, PR. China
**E-mail: hushaozheng001@163.com (S. H); lifayun15@hotmail.com (Z. F)*
Received August 3, 2012, Accepted September 17, 2012

The composite photocatalyst, N-TiO_2 loaded with Ni_2O_3, was prepared by N_2 plasma treatment. X-ray diffraction, X-ray fluorescence, N_2 adsorption, UV-vis spectroscopy, photoluminescence, and X-ray photoelectron spectroscopy were used to characterize the prepared TiO_2 samples. The results indicated that the band gap energy was decreased obviously by nitrogen doping, whereas loading of Ni_2O_3 did not influence the band gap and visible light absorption. The photocatalytic activities were tested in the degradation of 2,4,6-trichlorophenol (TCP) under visible light. The photocatalytic activity and stability of composite photocatalyst were much higher than that of catalyst modified with nitrogen or Ni_2O_3 alone. The synergistic effect of doping nitrogen and Ni_2O_3 over TiO_2 was investigated.

Key Words : TiO_2, TCP, Synergistic effect, Ni_2O_3, Stability

Introduction

The use of TiO_2 semiconductor photocatalyst to destroy organic compounds in contaminated air and water has been extensively studied in the last few years. Generally speaking, during irradiation of TiO_2 with ultraviolet (UV) light, a UV photon is absorbed by a TiO_2 particle, an electron (e^-)-hole (h^+) pair is generated. The e^- and h^+ may migrate to the surface of the photocatalyst particle and react with adsorbed reactants resulting in the desired process, or they may undergo undesired recombination.[1] However, TiO_2 can be activated only by UV irradiation, the amount of which corresponds to only 3% of total solar energy, for generation of photoexcited e^- and positive h^+.[2] Moreover, a large proportion of them recombine with each other without being utilized in chemical reactions. Thus, it is highly desirable to shift the absorption edge of TiO_2 to the visible-light region, and prevent recombination in order to make efficient use of the photoexcitation.

In the past decades, many efforts have been made to shift the absorption edge of TiO_2 to the visible-light region. It has been reported that TiO_2 doped with transition metals can absorb visible light.[3,4] However, the metal cation dopants often serve as recombination centers for the photogenerated electron-hole pairs, leading to a decreased activity.[5] Recently, the substitution of non-metal atoms, such as nitrogen,[6] sulfur,[7] phosphorous,[8] iodine,[9] and boron,[10] for oxygen in the lattice of TiO_2 was reported to enhance the catalytic activity of TiO_2 under visible light. But the synthesis of nonmetal-doped TiO_2 materials is much more difficult, because the lattice exchange requires high temperature and complicated procedures. More recently, much interest has been focused on the surface modification of TiO_2 with organic dyes for the construction of dye-sensitized photocatalytic systems under visible light irradiation.[11] Since the dye molecules are generally absorbed on rather than chemically bonded to the surface of TiO_2, a gradual decrease in photocatalytic activity has been observed. To increase the efficiency, the e^-/h^+ recombination rate needs to be reduced. Many efforts have been made in this direction. In general, there are three ways to achieve the separation of e^- and h^+. One is to modify TiO_2 by surface deposition of noble metal clusters.[12] The second is to couple TiO_2 with other semiconductors which can trap the photogenerated e^- or h^+.[13] The third alternative way is to introduce defects into the TiO_2 lattice by doping with transition metal ions, *e.g.* Fe^{3+} cations.[14]

Recently, ternary systems M, M'-TiO_2 (M, M' = metals and non-metals) for use as photocatalyst has been widely investigated. Sakatani *et al.*[15] reported that the N and La co-doped TiO_2 photocatalyst which prepared by means of polymerized method could degrade acetaldehyde under visible light irradiation. Zhao *et al.*[16] reported that the spectral response and photocatalytic efficiency could be improved by co-doping with nonmetal boron and the metal oxide Ni_2O_3. They suggested that incorporation of B into TiO_2 could extend the spectral response to the visible region and that the photocatalytic activity was greatly enhanced when it was further loaded with Ni_2O_3. Wei *et al.*[17] reported the preparation, characterization and photocatalytic activities of boron and cerium co-doped TiO_2 and pointed out that the photocatalytic activity of B-Ce codoped titania was much higher than that of P25.

Chlorophenols are deadly toxic compounds that present in waste water mainly arise from chemical intermediates or by products in petrochemical, paper making, plastic, pesticidal, and water disinfection. Moreover, chlorophenol is one of the most vulnerable water pollutants, which causes serious damage to the vital organs of human beings.[18,19] Thus, the removal of the chlorophenols from the waste water is highly imperative. It is widely accepted that N doping was one of

the most effective method to improve the visible light absorption.[6] Loading of Ni_2O_3 was proved to facilitate the excited electron transfer and hence suppress efficiently the recombination of photogenerated electron-hole.[20] Therefore, in this work, the composite photocatalyst, N-TiO_2 loaded with Ni_2O_3, was prepared by N_2 plasma treatment. The photocatalytic performance was evaluated in the degradation of TCP under visible light. The synergistic effect of doping nitrogen and Ni_2O_3 over TiO_2 was investigated.

Experimental

Preparation and Characterization. In a typical experiment, 0.1 mol of titanium isopropoxide was dissolved in 100 mL of anhydrous ethanol to form solution 1. A certain amount of nickelous nitrate (molar ratio Ni/Ti = 0.02) were dissolved in a mixture of 40 mL of deionized water adjusted to pH 2 with nitric acid and 60 mL of ethanol to prepare solution 2. Then, the solution 1 was added dropwise into the solution 2 within 60 min under vigorous stirring at room temperature to form the sol, followed by stirring continuously for 5 h and aging for 3 d at room temperature to prepare the gel. The obtained gel was dried for 10 h at 80 ºC, followed by milling and annealing at 500 ºC for 2 h to remove the residual organic compounds (at a rate of 5 ºC/min). The obtained product was denoted as Ni_2O_3/TiO_2. For comparison, neat TiO_2 was prepared following the same procedure as in the synthesis of Ni_2O_3/TiO_2 but in the absence of nickelous nitrate.

The N doping was conducted in a dielectric barrier discharge (DBD) reactor, consisting of a quartz tube and two electrodes. The high-voltage electrode was a stainless-steel rod (2.5 mm), which was installed in the axis of the quartz tube and connected to a high voltage supply. The grounding electrode was an aluminum foil which was wrapped around the quartz tube. For each run, 0.4 g prepared Ni_2O_3/TiO_2 was charged into the quartz tube. At a constant N_2 flow (50 mL min^{-1}), a high voltage of 10 kV was supplied by a plasma generator at an overall power input of 50 V × 0.4 A. The discharge frequency was fixed at 10 kHz, and the discharge was kept for 6 min. After discharge, the reactor was cooled down to room temperature. The obtained material was denoted as Ni_2O_3/N-TiO_2. When neat TiO_2 was used to replace Ni_2O_3/TiO_2 following the same procedure as in the synthesis of Ni_2O_3/N-TiO_2, the product is denoted as N-TiO_2. The mechanical mixing sample, Ni_2O_3-N-TiO_2, was obtained for comparison by mixing the prepared N-TiO_2 and commercial Ni_2O_3 with the same Ni/Ti ratio to Ni_2O_3/N-TiO_2.

XRD patterns of the prepared TiO_2 samples were recorded on a Rigaku D/max-2400 instrument using Cu-Kα radiation (λ = 1.54 Å). Quantitative X-ray fluorescence analysis (XRF) was performed by using an X-ray fluorescence spectrometer (SXF-1200 analyzer). UV-vis spectroscopy measurement was carried out on a Jasco V-550 spectrophotometer, using $BaSO_4$ as the reference sample. The Brunauer-Emmett-Teller (BET)-specific surface areas (S_{BET}) of the samples were determined through nitrogen adsorption at 77 K (Micromeritics ASAP 2010). All the samples were degassed at 393 K before the measurement. Photoluminescence (PL) spectra were measured at room temperature with a fluorospectrophotometer (FP-6300) using an Xe lamp as excitation source. XPS measurements were conducted on a Thermo Escalab 250 XPS system with Al Kα radiation as the exciting source. The binding energies were calibrated by referencing the C 1s peak (284.6 eV) to reduce the sample charge effect.

Photocatalytic Reaction. Suspensions were prepared in deionised water by mixing TiO_2 catalyst with appropriate solutions of TCP. In a typical procedure, 0.1 g TiO_2 powders were dispersed in 100 mL solution of TCP (initial concentration $C_0 = 60 \times 10^{-6}$ g·mL^{-1}) in an ultrasound generator for 10 min. The suspension was transferred into a self-designed glass reactor, and stirred for 30 min in darkness to achieve the adsorption equilibrium. The concentration of TCP at this point was considered as the absorption equilibrium concentration $C_{0'}$. The adsorption capacity of a catalyst to TCP was defined by the adsorption amount of TCP on the photocatalyst (C_0-$C_{0'}$). In the photoreaction under visible light irradiation, the suspension was exposed to a 110-W high-pressure sodium lamp with main emission in the range of 400-800 nm, and air was bubbled at 130 mL/min through the solution. The UV light portion of sodium lamp was filtered by 0.5 M $NaNO_2$ solution. All runs were conducted at ambient pressure and 30 ºC. The conversion of TCP was determined using an Agilent 1100 series HPLC operated in isocratic mode under the following conditions: methanol-water (80%:20%); flow rate 1 mL·min^{-1}; temperature 25 ºC; Column Phenomenex Luna 10 μ Phenyl-Hexyl, 4.6 mm × 250 mm; detector UV at 254 nm; injection volume 5 μL.

Results and Discussion

The XRD patterns of neat TiO_2, N-TiO_2, Ni_2O_3/TiO_2, and Ni_2O_3/N-TiO_2 are shown in Figure 1. All the samples were anatase phase. There was no observable structural difference between neat and modified TiO_2 samples. The lattice parameters of the catalysts were measured using (1 0 1) and (2 0 0) in anatase crystal planes by using equations:[21]

$$d_{(hkl)} = \frac{\lambda}{2\sin\theta} \quad (1)$$

$$d_{(hkl)}^{-2} = h^2 a^{-2} + k^2 b^{-2} + l^2 c^{-2} \quad (2)$$

where $d_{(h\,k\,l)}$ is the distance between crystal planes of (h k l), λ is the X-ray wavelength, θ is the diffraction angle of crystal plane (h k l), h k l is the crystal index. The a, b and c are lattice parameters (in anatase form, $a = b \neq c$). The results shown in Table 1 indicated that the lattice parameters of all samples remain almost unchanged along a- and b-axes, whereas the c-axis parameter decreased for N_2-plasma treated samples, N-TiO_2 and Ni_2O_3/N-TiO_2. This indicated that N atoms doped into the TiO_2 lattice, leading to the decrease in the cell volume. Besides, for Ni_2O_3/TiO_2, no obvious change in lattice parameters were observed, indicating Ni is not

Table 1. Summary of physical properties of prepared TiO_2 samples

Sample	Size (nm)	S_{BET} (m^2g^{-1})	Lattice parameters a = b, c (Å)	E_g (eV)
TiO_2	15.6	69.8	0.37835, 0.95105	3.07
N-TiO_2	13.8	82.5	0.37851, 0.94736	2.87
Ni_2O_3/TiO_2	9.5	110.3	0.37829, 0.95158	3.04
Ni_2O_3/N-TiO_2	8.2	122.7	0.37818, 0.94728	2.82

weaved into the crystal structure and is separated from the phase. However, no other crystalline phase containing Ni was observed. Therefore, it is deduced that very fine dispersion of Ni_2O_3 loaded in the titania which is below the detection limit of this technique. Besides, the particle sizes of the samples were calculated by their XRD patterns according to the Debye-Scherrer equation,[22] and shown in Table 1. Obviously, the particle size decreased for the Ni_2O_3 loaded samples. This is probably due to that the coverage of TiO_2 surface by Ni_2O_3, leading to the restriction of grain growth.

Figure 2 shows the XP spectra of neat TiO_2, N-TiO_2, Ni_2O_3/TiO_2, and Ni_2O_3/N-TiO_2. In the Ti 2p region (Fig. 2(a)), both samples exhibited two peaks which could be assigned to Ti^{4+} $2p_{3/2}$ and Ti^{4+} $2p_{1/2}$. The binding energy differences, ΔE = $E(Ti^{4+}\ 2p_{1/2}) - E(Ti^{4+}\ 2p_{3/2})$, for both samples were around 5.7 eV, which is consistent with previous literature.[23] Besides, compared with neat TiO_2, slight shifts to lower binding energies were observed for Ni_2O_3/N-TiO_2 in the region of Ti 2p and O 1s (Fig. 2(a), (b)). This is probably attributed to change

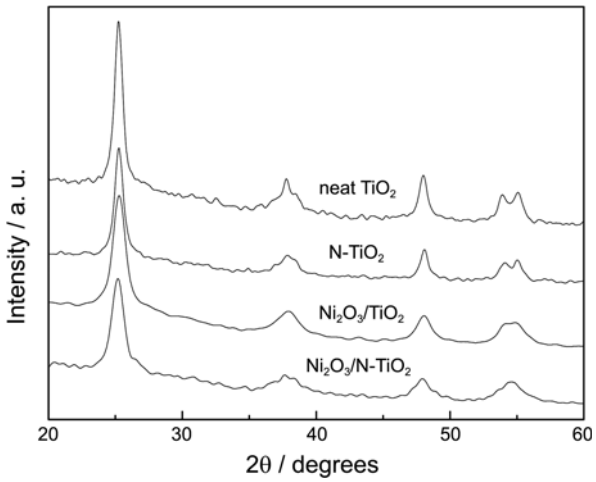

Figure 1. XRD patterns of neat TiO_2, N-TiO_2, Ni_2O_3/TiO_2, and Ni_2O_3/N-TiO_2.

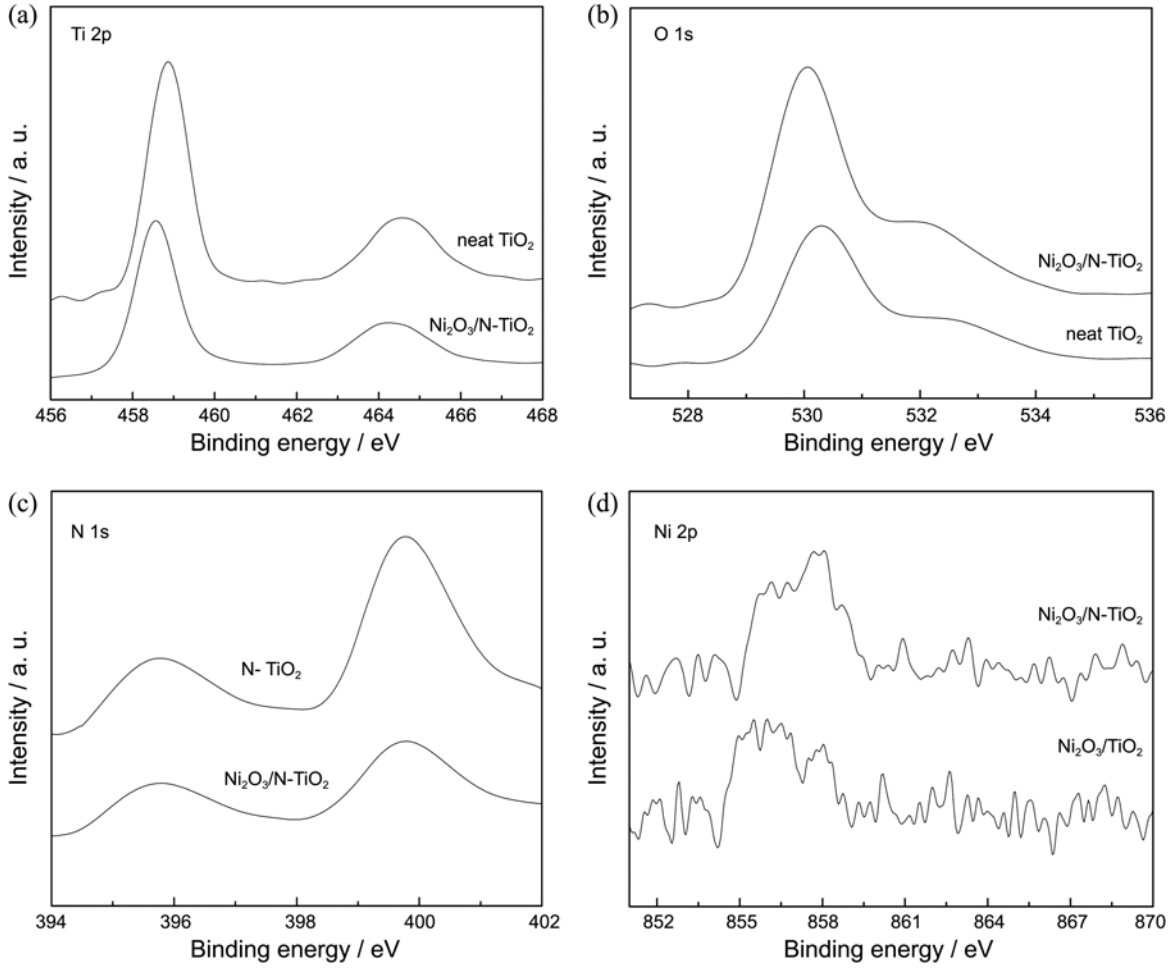

Figure 2. XP spectra of neat TiO_2, N-TiO_2, Ni_2O_3/TiO_2, and Ni_2O_3/N-TiO_2 in the region of Ti 2p (a), O 1s (b), N 1s (c), and Ni 2p (d).

of chemical environment after N doping. The electrons of N atoms may be partially transferred from N to Ti and O, due to the higher electronegativity of oxygen, leading to increased electron density on Ti and O atoms. In the region of O 1s (Fig. 2(b)), the XPS peaks around 529.9 and 531.8 eV are attributed to crystal lattice oxygen (Ti-O) and surface hydroxyl group (O-H) of TiO_2.[24] The ratio of these two peak areas ($S_{O\text{-}H}/S_{Ti\text{-}O}$) represents the abundance of surface hydroxyl groups. The $S_{O\text{-}H}/S_{Ti\text{-}O}$ ratios for neat TiO_2 and Ni_2O_3/N-TiO_2 were 0.12 and 0.23, respectively. This indicated that Ni_2O_3/N-TiO_2 sample with smaller particle size could absorb more surface hydroxyl group, which play crucial roles in photocatalytic reactions.

In the N 1s region (Fig. 2(c)), the peaks around 396 and 400 eV are observed in both samples, which are attributed to the formation of lattice-nitrogen and other surface N species such as N-N and N-O bond, respectively. This is consistent with our previous results.[25] Yamada *et al.*[26] prepared N doped TiO_2 by N_2 plasma method. They suggested that the scission of Ti-O bond on TiO_2 surface took place under the nitrogen plasma state, which had a high electron temperature (5-6 eV). Thus, nitrogen atoms will replace lattice oxygen easily. No obvious difference in binding energy between N-TiO_2 and Ni_2O_3/N-TiO_2 was observed, indicating loading of Ni_2O_3 did not influence the doping of N. In the region of Ni 2p (Fig. 2(d)), the binding energy for the broad peak was around 856.0 eV, which assigned to Ni $2p_{3/2}$ in Ni_2O_3 according to the literature.[27] This proved that Ni was existed as Ni_2O_3 in the catalyst, which is consistent with XRD result. The molar ratio of Ni/Ti on the TiO_2 surface was 0.044, calculated according to the XPS data. However, the XRF result indicated that the molar ratio of Ni/Ti in the bulk was 0.018, which is coincident with the experimental method. This confirmed that Ni_2O_3 existed mostly on the TiO_2 surface. Besides, it should be noted that the binding energy for Ni_2O_3/TiO_2 shifted slightly after N_2 plasma treatment. This is probably due to the formation of interaction between Ni_2O_3 and TiO_2 caused by the plasma treatment, leading to the change of chemical environment of Ni. The surface hydroxyl group of TiO_2 was probably activated by the plasma treatment, and bond with Ni, leading to the lower electron density. Thus, the binding energy of Ni 2p increased slightly after plasma treatment.

UV-Vis spectra for neat TiO_2, N-TiO_2, Ni_2O_3/TiO_2, and Ni_2O_3/N-TiO_2 are shown in Figure 3. It could be seen that there were strong absorptions in the visible light region and that the absorption edges were shifted to the lower energy region for the sample of N-TiO_2 and Ni_2O_3/N-TiO_2, whereas no absorption in visible light region for the sample of neat TiO_2 and Ni_2O_3/TiO_2 was observed. The red shift of the absorption edge implied a decrease in the band gap energy. In order to calculate the onsets of absorption edges, a tangent was drawn on absorption spectra and was extrapolated, and the intercept on the wavelength axis was obtained. The results were 402.5, 408, 432.4, and 439 nm for the sample of neat TiO_2, Ni_2O_3/TiO_2, N-TiO_2, and Ni_2O_3/N-TiO_2, respectively. Therefore, the band gap energies could be calculated according to the method of Oregan and Gratzel,[28] and the values were 3.07, 3.04, 2.87, and 2.82 eV for neat TiO_2, Ni_2O_3/TiO_2, N-TiO_2, and Ni_2O_3/N-TiO_2 (Table 1). These results clearly indicated that the band gap energy was decreased obviously by nitrogen doping, whereas loading of Ni_2O_3 did not influence the band gap and visible light absorption.

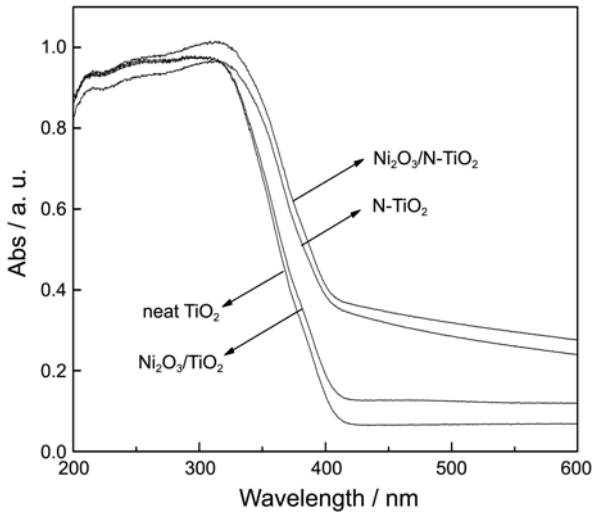

Figure 3. UV-vis spectra of neat TiO_2, N-TiO_2, Ni_2O_3/TiO_2, and Ni_2O_3/N-TiO_2.

Table 2. Comparison of lattice-nitrogen stability in N-TiO_2 and Ni_2O_3/N-TiO_2

Sample	Fresh catalyst (at %)	1st reuse (at %)	2nd reuse (at %)	3rd reuse (at %)
N-TiO_2	0.28	0.22	0.19	0.16
N-TiO_2 + KI (0.1 M)	0.27	0.26	0.25	0.25
Ni_2O_3/N-TiO_2	0.25	0.24	0.23	0.23

The PL technique has been useful in the field of photocatalysis over semiconductors for understanding the surface processes. PL spectrum is an effective way to study the electronic structure, optical and photochemical properties of semiconductor materials, by which information such as surface oxygen vacancies and defects, as well as the efficiency of charge carrier trapping, immigration and transfer can be obtained.[29] It is well known that the PL signals of semiconductor materials result from the recombination of photo-induced charge carriers. In general, the lower the PL intensity, the lower the recombination rate of photo-induced electron-hole pairs, thus the higher the photocatalytic activity. Figure 4 shows the PL spectra of prepared TiO_2 samples, using excitation at 320 nm. Compared with neat TiO_2, the PL intensities decreased slightly after N doping (N-TiO_2). However, for Ni_2O_3 loaded samples, the PL intensities decreased markedly. It is known that most of the electrons and holes recombine within a few nanoseconds in the absence of scavengers. If scavengers or surface defects are present to trap the electrons or holes, the electron-hole recombination can be suppressed. Ganesh *et al.*[30,31] prepared the nickel ions modified Fe/TiO_2 catalyst, and found the presence of Ni^{2+}

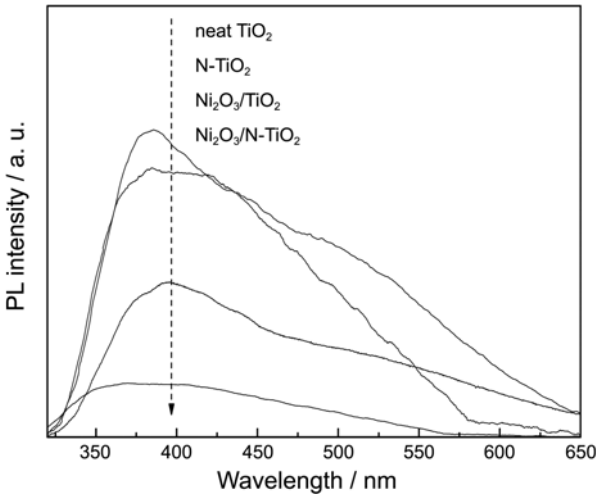

Figure 4. PL spectra of neat TiO_2, N-TiO_2, Ni_2O_3/TiO_2, and Ni_2O_3/N-TiO_2.

and Ni^{3+} by EPR. They considered that Ni^{3+} will trap the photogenerated electron to form Ni^{2+} during the irradiation process. Therefore, in this investigation, Ni_2O_3 will trap the photogenerated electron, hence suppress efficiently the recombination of photogenerated electron-hole.[20] Besides, it is shown that PL intensity of Ni_2O_3/N-TiO_2 was much lower than that of Ni_2O_3/TiO_2 sample. This indicated that the recombination of photogenerated electron-hole for Ni_2O_3/TiO_2 sample decreased after plasma treatment. It has been proved that N doping slightly decreased the PL intensity, indicating inapparent influence on recombination. Therefore, such difference in recombination rate should be attributed to the interaction between Ni_2O_3 and TiO_2 after plasma treatment (Fig. 2(d)), leading to the electron transfer more effectively in Ni_2O_3/N-TiO_2.

The adsorption of TCP on TiO_2-based catalysts was measured by the equilibrium adsorption capacity. Compared with neat TiO_2, slight decrease in the adsorption capacity was shown for N-TiO_2, whereas the adsorption capacity of Ni_2O_3 loaded TiO_2 samples increased markedly (Fig. 5). It is reported that such decreased adsorption capacity is attributed to the coverage of TiO_2 surface by excess surface N species (Fig. 2(c)), leading to the reduced surface sites for adsorbing.[32] The BET specific surface areas (S_{BET}) of prepared samples are listed in Table 1. It is obvious that the S_{BET} increased with the decreased particle size. The S_{BET} of Ni_2O_3/TiO_2 and Ni_2O_3/N-TiO_2 were much higher than that of samples without Ni_2O_3 loading. Such increased S_{BET} for Ni_2O_3/TiO_2 and Ni_2O_3/N-TiO_2 lead to the increased equilibrium adsorption capacity.

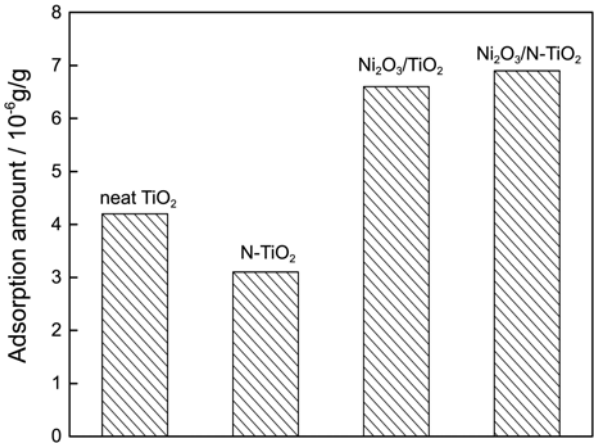

Figure 5. Adsorption capacity of TCP on neat TiO_2, N-TiO_2, Ni_2O_3/TiO_2, and Ni_2O_3/N-TiO_2.

The photocatalytic activities of prepared TiO_2 samples under visible light are shown in Figure 6. It is shown that neat TiO_2 and Ni_2O_3/TiO_2 exhibited no activity, agreeing well with the result from the UV-vis analysis that the two samples had no response to visible light. After N doping, obvious improvement in photocatalytic activities were observed. Those enhanced photocatalytic activities must result from the doping of nitrogen in TiO_2, which gave rise to the enhanced absorption in the visible region. Compare the N doped samples, it is observed that Ni_2O_3/N-TiO_2 exhibited the highest activity, whereas N-TiO_2 and Ni_2O_3-N-TiO_2 showed almost the same activity. This must result from the interaction between Ni_2O_3 and TiO_2 caused by plasma treatment, which accelerate the excited electron transfer and hence suppress efficiently the recombination of photoproduced electron-hole, increase photo quantum efficiency. Therefore, the activity of Ni_2O_3/N-TiO_2 was much higher than that of N-TiO_2. For Ni_2O_3-N-TiO_2, mechanical mixing sample, the large intermolecular distance between Ni_2O_3 and TiO_2 cause no interaction between them, leading to the same activity with N-TiO_2.

In our previous report, it is concluded that the optimal discharge time was 6 min for N doping. When the discharge time beyond 6 min, the excess surface N species cover the TiO_2 surface, cause a dramatic decrease of equilibrium adsorption capacity, thus leading to the activity decrease.[32] Therefore, in this investigation, the discharge time was 6 min. Besides the nitridation condition, the Ni_2O_3 content plays an important role in the photocatalytic activity. In

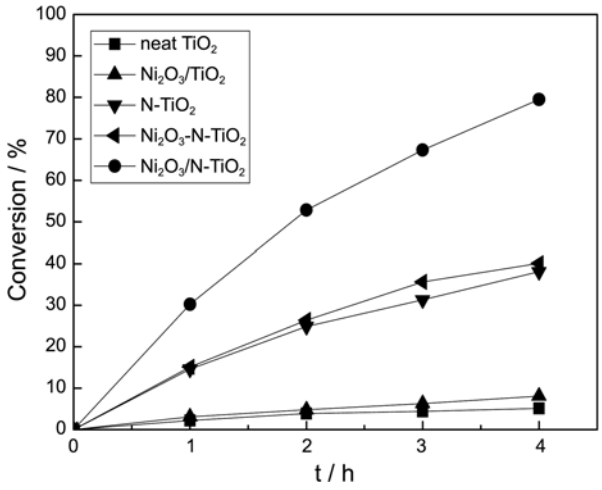

Figure 6. Photocatalytic performances of prepared samples in the degradation TCP under visible light irradiation.

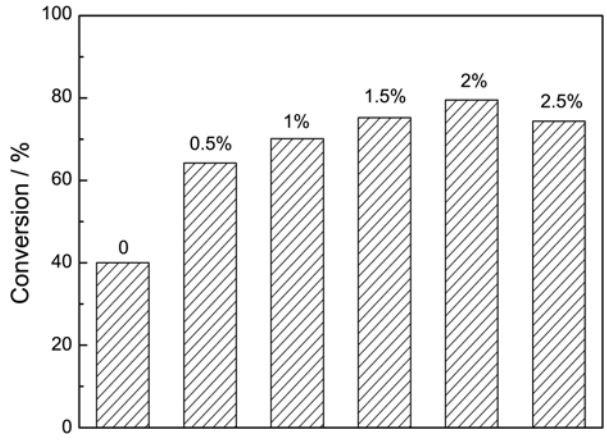

Figure 7. The effect of Ni_2O_3 content on the photocatalytic performance.

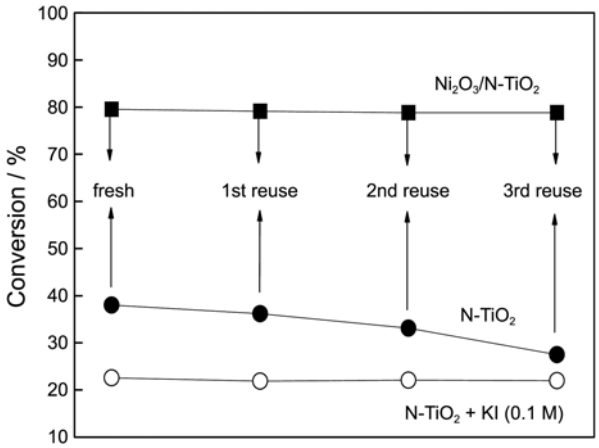

Figure 8. Photocatalytic stability of N-TiO_2 and Ni_2O_3/N-TiO_2 in the degradation of TCP.

Figure 7, the effect of Ni_2O_3 content on the photocatalytic performance, it is shown that the photocatalytic activity of the catalyst without Ni_2O_3 loading was lower than 40%. After loading with Ni_2O_3, the activities increased obviously. However, when the atomic ratio of Ni to Ti beyond 0.02, the photoactivity decreased. Therefore, the optimum atomic ratio of Ni to Ti was 0.02. In fact, the appropriate amount of Ni_2O_3 could suppress the recombination of e^-/h^+ whereas the excess amounts of Ni_2O_3 might cover the surface of TiO_2, increased the number of recombination centers, decreased the photo quantum efficiency and led to low photoactivity.

The photocatalytic performances of N-TiO_2 and Ni_2O_3/N-TiO_2 were investigated in three cycles to check the photocatalytic stability (Fig. 8). It is shown that the activity of Ni_2O_3/N-TiO_2 decreased slightly after three reuse (79.5% to 78.8%), whereas the continuous decrease was shown in N-TiO_2, from 38% for fresh catalyst to 27.5% for 3rd reused catalyst. Chen *et al.*[33] reported that the lattice-nitrogen was oxidated by photogenerated holes during the degradation reaction, cause the decrease of lattice-nitrogen content, thus leading to the poor stability. Therefore, the lattice-nitrogen contents of fresh and reused N-TiO_2 and Ni_2O_3/N-TiO_2 are calculated according to the relevant XPS data and shown in Table 2. For N-TiO_2, continuous decrease in lattice-nitrogen content was observed, which is consistent with the result of Chen.[33] However, the lattice-nitrogen content of Ni_2O_3/N-TiO_2 kept stable in the three cycles. Rabani *et al.*[34] used iodide ion as scavenger to investigate the effect of h^+ on the photocatalytic process. Therefore, in this investigation, 0.1 M KI was added to check whether lattice-nitrogen was oxidated by photogenerated h^+. The result shown in Figure 8 indicated that the activity of N-TiO_2 decreased whereas the photocatalytic stability improved obviously when KI was added. Besides, the lattice-nitrogen stability of N-TiO_2 shown in Table 2 also improved after KI addition. This confirmed the loss of lattice-nitrogen was due to the oxidation by photogenerated h^+. It is reported that the Ni^{3+} will trap the photogenerated electron to form Ni^{2+} during the irradiation process, thus decrease the recombination rate.[30,31] Then, the formed Ni^{2+} will react with photogenerated h^+ and back to Ni^{3+} (Eq. 3, 4).[35,36] Therefore, it is deduced that loading of Ni_2O_3 not only facilitate the excited electron transfer and increase the photo quantum efficiency, but also played the role of nitrogen stabilizer, restrained the oxidation of lattice-nitrogen by trapping the photogenerated h^+, thus improve the photocatalytic activity and stability.

$$Ni^{3+} + e^- \rightarrow Ni^{2+} \quad (3)$$

$$Ni^{2+} + h^- \rightarrow Ni^{3+} \quad (4)$$

Conclusion

The composite photocatalyst, N-TiO_2 loaded with Ni_2O_3, was prepared by N_2 plasma treatment. The coverage of TiO_2 surface by Ni_2O_3 caused the restriction of grain growth, thus leading to the decreased particle size. The band gap energy was decreased obviously by nitrogen doping, whereas loading of Ni_2O_3 did not influence the band gap and visible light absorption. Some interaction between Ni_2O_3 and TiO_2 was formed by N_2 plasma treatment, leading to the accelerated electron transfer from TiO_2 to Ni_2O_3, hence suppress efficiently the recombination of photoproduced electron-hole. Besides, the photocatalytic stability of N doped TiO_2 catalyst was obviously improved by Ni_2O_3 loading. This indicated that loading of Ni_2O_3 not only facilitate the excited electron transfer and increase the photo quantum efficiency, but also played the role of nitrogen stabilizer, thus improve the photocatalytic activity and stability.

Acknowledgments. This work was supported by National Natural Science Foundation of China (No. 41071317, 30972418), National Key Technology R & D Programme of China (No. 2007BAC16B07, 2012ZX07505-001), the Natural Science Foundation of Liaoning Province (No. 20092080).

References

1. Wang, C. Y.; Bottcher, C.; Bahnemann, D. W.; Dohrmann, J. K. *J. Mater. Chem.* **2003**, *13*, 2322.

2. Hoffmann, M. R.; Martin, S. T.; Choi, W.; Bahnemann, D. W. *Chem. Rev.* **1995**, *95*, 69.
3. Klosek, S.; Raftery, D. *J. Phys. Chem. B.* **2001**, *105*, 2815.
4. Yamashita, H.; Harada, M.; Misaka, J.; Takeuchi, M.; Ikeue, K.; Anpo, M. *J. Photochem. Photobiol. A: Chem.* **2002**, *148*, 257.
5. Choi, W.; Termin, A.; Hoffmann, M. R. *J. Phys. Chem.* **1994**, *98*, 13669.
6. Asahi, R.; Morikawa, T.; Ohwaki, T.; Aoki, A.; Taga, Y. *Science* **2001**, *293*, 269.
7. Sun, H. J.; Liu, H. L.; Ma, J.; Wang, X. Y.; Wang, B.; Han, L. *J. Hazard. Mater.* **2008**, *156*, 552.
8. Shi, Q.; Yang, D.; Jiang, Z. Y.; Li, J. *J. Mol. Catal. B: Enzym.* **2006**, *43*, 44.
9. Abe, R.; Sayama, K.; Domen, K.; Arakawa, H. *Chem. Phys. Lett.* **2001**, *344*, 339.
10. Zaleska, A.; Sobczak, J. W.; Grabowska, E.; Hupka, J. *Appl. Catal. B: Environ.* **2008**, *78*, 92.
11. Chatterjee, D. ; Mahata, A. *Appl. Catal. B: Environ.* **2001**, *33*, 119.
12. Wang, C. Y.; Liu, C. Y.; Zheng, X.; Chen, J.; Shen, T. *Colloids Surf. A Physicochem. Eng. Asp.* **1998**, *131*, 271.
13. Cao, Y.; Zhang, X.; Yang, W.; Du, H.; Bai, Y.; Li, T.; Yao, J. *Chem. Mater.* **2000**, *12*, 3445.
14. Soria, J.; Conesa, J. C.; Augugliaro, V.; Palmisano, L.; Schiavello, M.; Sclafani, A. *J. Phys. Chem.* **1991**, *95*, 274.
15. Sakatani, Y.; Nunoshige, J.; Ando, H.; Okusako, K.; Koike, H.; Takata, T.; Kondo, J. N.; Hara, M.; Domen, K. *Chem. Lett.* **2003**, *32*, 1156.
16. Zhao, W.; Ma, W. H.; Chen, C. C.; Zhao, J. C.; Shuai, Z. G. *J. Am. Chem. Soc.* **2004**, *126*, 4782.
17. Wei, C. H.; Tang, X. H.; Liang, J. R.; Tan, S. Y. *J. Environ. Sci.-China* **2007**, *19*, 90.
18. D'Olivera, J. C.; Al-sayed, G.; Pichat, P. *Environ. Sci. Technol.* **1990**, *24*, 990.
19. Keith, L. H.; Telliard, W. A. *Environ. Sci. Technol.* **1979**, *13*, 416.
20. Zou, Z. G.; Ye, J. H.; Sayama, K.; Arakawa, H. *Nature* **2001**, *414*, 625.
21. Shen, X. Z.; Liu, Z. C.; Xie, S. M.; Guo, J. *J. Hazard. Mater.* **2009**, *162*, 1193.
22. Lin, J.; Lin, Y.; Liu, P.; Meziani, M. J.; Allard, L. F.; Sun, Y. P. *J. Am. Chem. Soc.* **2002**, *124*, 11514.
23. Yu, J. G.; Zhao, X. J.; Zhao, Q. N. *Mater. Chem. Phys.* **2001**, *69*, 25.
24. Xu, J. J.; Ao, Y. H.; Fu, D. G.; Yuan, C. W. *J. Cryst. Growth* **2008**, *310*, 4319.
25. Hu, S. Z.; Li, F. Y.; Fan, Z. P. *Bull. Korean Chem. Soc.* **2012**, *33*, 199.
26. Yamada, K.; Nakamura, H.; Matsushima, S.; Yamane, H.; Haishi, T.; Ohira, K.; Kumada, K. *C. R. Chimie* **2006**, *9*, 788.
27. Kosaku, K. *J. Electron Spectrosc. Relat. Phenom.* **1988**, *46*, 237.
28. Oregan, B.; Gratzel, M. *Nature* **1991**, *353*, 737.
29. Cong, Y.; Zhang, J.; Chen, F.; Anpo, M. *J. Phys. Chem. C* **2007**, *111*, 6976.
30. Ganesh, K. P.; Ruey-an, D. *Appl. Catal. B: Environ.* **2010**, *100*, 116.
31. Ganesh, K. P.; Ruey-an, D. *Water Res.* **2011**, *45*, 4198.
32. Hu, S. Z.; Li, F. Y.; Fan, Z. P. *Appl. Surf. Sci.* **2011**, *258*, 1249.
33. Chen, X. F.; Wang, X. C.; Hou, Y. D.; Huang, J. H.; Wu, L.; Fu, X. Z. *J. Catal*. **2008**, *255*, 59.
34. Rabani, J.; Yamashita, K.; Ushida, K.; Stark, J.; Kira, A. *J. Phys. Chem. B* **1998**, *102*, 1689.
35. Devi, L. G.; Kottam, N.; Murthy, B. N.; Kumar, S. G. *J. Mol. Catal. A: Chem.* **2010**, *328*, 44.
36. Devi, L. G.; Kottam, N.; Kumar, N. S. G.; Raiashekhar, K. E. *Cent. Eur. J. Chem.* **2010**, *8*, 142.